journal

J. Am. Ceram. Soc., 84 [5] 1087–92 (2001)

Crystallization of Sol–Gel-Derived Barium Strontium Titanate Thin Films

Maria C. Gust,*,† Leslie A. Momoda,‡ Neal D. Evans,§ and Martha L. Mecartney*,†

Department of Chemical and Biochemical Engineering and Materials Science, University of California, Irvine, California 92697-2575; Hughes Research Laboratories, Malibu, California 90265; and Oak Ridge Institute for Science and Education, Oak Ridge, Tennessee 37831-0117

Microstructural development of thin-film barium strontium titanate ($Ba_xSr_{1-x}TiO_3$) as a function of strontium concentration and thermal treatment were studied, using transmission electron microscopy (TEM) and X-ray diffractometry (XRD). Thin films, ~250 nm thick, were spin-coated onto Pt/Ti/SiO_2/Si substrates, using methoxypropoxide alkoxide precursors, and crystallized by heat-treating at 700°C. All films had the cubic perovskite structure, and their lattice parameters varied linearly with strontium content. Films with higher strontium concentrations had a larger average grain size. *In situ* TEM heating experiments, combined with differential thermal analysis/thermogravimetric analysis results, suggest that the gel films crystallize as an intermediate carbonate phase, $Ba_xSr_{1-x}TiO_2CO_3$ (with a solid solution range from $x = 1$ to $x = 0$). Before decomposition at 600°C, this carbonate phase inhibits the formation of the desired perovskite phase.

I. Introduction

THE trend toward increased storage densities in electronic devices such as dynamic random access memory (DRAM) necessitates the use of capacitors with high dielectric constants.[1] One potentially suitable material for these applications is $Ba_xSr_{1-x}TiO_3$. The Curie temperature of $Ba_xSr_{1-x}TiO_3$ decreases linearly with increasing amounts of strontium in the $BaTiO_3$ lattice, which enables the ferroelectric/paraelectric transition temperature to be tailored for specific applications by varying the strontium content. The Curie temperature for bulk $Ba_{0.7}Sr_{0.3}TiO_3$ is ~25°C.

Methods such as laser ablation,[2–4] sputtering,[5–7] and metallorganic chemical vapor deposition (MOCVD)[8] have been used to deposit $Ba_xSr_{1-x}TiO_3$ thin films. Wet chemical methods such as metallorganic deposition (MOD)[9,10] and sol–gel[11–14] have also been used to prepare $Ba_xSr_{1-x}TiO_3$ thin films. The wet chemical methods have advantages over other thin-film deposition techniques in that better compositional control and better homogeneity can more easily be achieved. In addition, the process may be more economical for production, because no high vacuum systems are needed.

In this work, the effects of variations in the strontium concentration on the microstructure of methoxypropoxide-derived $Ba_xSr_{1-x}TiO_3$ films were investigated. The crystallization behavior of $Ba_{0.5}Sr_{0.5}TiO_3$ was also studied, using *in situ* transmission electron microscopy (TEM) heating experiments to evaluate the evolution of the thin-film microstructure. The overall goal of this research is to better understand the role that process parameters, such as strontium concentration, play in controlling the microstructural development.

II. Experimental Procedure

Sols for $Ba_xSr_{1-x}TiO_3$ ($x = 1$, 0.75, 0.65, 0.50, 0.25, and 0) were prepared by refluxing the appropriate amounts of Ba-Ti and Sr-Ti methoxypropoxide (Gelest, Tullytown, PA) in butanol for 18 h. Butanol and water for hydrolysis (0.5 mol water/mol alkoxide) were added to bring the sols to a final concentration of 0.25*M*. Higher concentrations of water caused the sols to precipitate within minutes.

Thin films were prepared by spin-coating the sols onto Pt/Ti/SiO_2/Si (100) substrates at 2000 rpm for 1 min. After deposition of each layer, films were pyrolized at 350°C for 5 min, to burn off residual organics, followed by a crystallization heat treatment at 700°C for 30 min in flowing oxygen. The films were inserted when the furnace was at temperature. To build up the film thickness, five layers were deposited onto each substrate, for a total film thickness between 230 and 260 nm.

The crystallization of the $Ba_xSr_{1-x}TiO_3$ films was studied using glancing-angle thin-film X-ray diffractometry (XRD; Model D5000, Siemens Aktiengesellschaft, Karlsruhe, Germany), with incident X rays at an angle of 2° to the film surface. This technique is most useful for diffraction analysis of thin films with minimal volume for analysis. CuK_α radiation was used. Microstructural characterization of the films was conducted using an analytical TEM (Model CM20, Philips Research Laboratories, Eindhoven, The Netherlands) operated at 200 kV. Conventional dimpling and ion-milling techniques were used to prepare films for TEM investigation.

Differential thermal analysis (DTA) and thermogravimetric analysis (TGA) (Model 2100 Thermal Analysis System, E. I. du Pont de Nemours & Co., Inc., Wilmington, DE) were used to determine the thermochemical properties of dried gel powders. Sols were dried in a vacuum furnace at 100°C and crushed to fine powder, using a mortar and pestle. DTA and TGA studies were conducted by heating the dried powders in oxygen, at 10°C/min, to 1000°C.

In situ TEM heating experiments were conducted on amorphous $Ba_{0.5}Sr_{0.5}TiO_3$ thin films. To prepare films for *in situ* heating, five layers were spin-coated onto each substrate, with a pyrolysis heat treatment at 350°C after each layer. Thin TEM foils of pyrolyzed films were then prepared, using conventional dimpling and ion milling. The *in situ* TEM hot-stage experiments were conducted using a Philips CM30 operated at 300 kV and a single-tilt Gatan heating holder (Model 628-0500 Hot Stage Power Supply, Gatan,

B. A. Tuttle—contributing editor

Manuscript No. 188663. Received March 24, 2000; approved November 22, 2000.
Supported by the State of California MICRO Program, Research Project No. 95-103, in collaboration with Hughes Research Laboratories, and by the Division of Materials Science, U. S. Department of Energy, under Contract No. DE-AC05-96OR22464, with Lockheed Martin Energy Research Corporation, and through the DOE-sponsored SHaRE Program, under Contract No. DE-AC05-76OR00033, with Oak Ridge Associated Universities.

*Member, American Ceramic Society.
†University of California.
‡Hughes Research Laboratories.
§Oak Ridge Institute for Science and Education.

Inc., Pleasanton, CA). Samples were initially heated to 300°C in the microscope and held at this temperature for ~5 min, to burn off water and contaminants. The holder temperature was then raised to the desired annealing temperature within a couple of minutes. To minimize electron-beam damage, the beam was kept off the area of interest except when photographs were being taken.

III. Results

(1) Effects of Strontium Concentration

The XRD patterns of the $Ba_xSr_{1-x}TiO_3$ films are shown in Fig. 1. With the exception of the platinum peaks from the substrate, all other peaks were identified as perovskite $Ba_xSr_{1-x}TiO_3$ (BST). These *d* spacings were used to determine the lattice parameter for each of the compositions (Fig. 2). All compositions were assumed to be cubic, and no evidence for tetragonality was seen in the $BaTiO_3$ and $Ba_{0.75}Sr_{0.25}TiO_3$ films. (There was no evidence of peak splitting in XRD, and no ferroelectric domains were observed by TEM.) The lattice parameter decreased linearly with increasing strontium concentration.

Bright-field TEM micrographs and corresponding electron diffraction patterns of films representing each composition after the 700°C heat treatment are shown in Fig. 3. The films were single-phase, randomly oriented polycrystalline $Ba_xSr_{1-x}TiO_3$. All films contained residual porosity. The grain size increased with increasing strontium concentration, as reflected in the increasing discontinuity in the diffraction rings using the same selected-area aperture of 10 μm. The average grain sizes for $Ba_xSr_{1-x}TiO_3$ with $x = 1$, 0.75, 0.65, 0.50, 0.25, and 0 were ~40, 50, 60, 70, 110, and 120 nm, respectively. In addition to an increase in grain size, an increase in the grain-size distribution was seen as the strontium concentration increased, from 20 to 60 nm for $BaTiO_3$ to 20–220 nm for $SrTiO_3$. The representative cross sections in the micrographs of Fig. 4 show that some of the large grains were located near the film/platinum interface and that some large grains extended all the way through the thickness of the film.

The DTA and TGA results of $BaTiO_3$, $Ba_{0.5}Sr_{0.5}TiO_3$, and $SrTiO_3$ dried gels are shown in Fig. 5. All dried gel powders exhibited a large weight loss at ~600°C. The weight loss was 16.9%, 17.5%, and 18.6% for $BaTiO_3$, $Ba_{0.5}Sr_{0.5}TiO_3$, and $SrTiO_3$, respectively. Note that the percent weight loss associated with this particular decomposition reaction should be equal to the weight at 600°C (before the decomposition reaction) minus the weight after the decomposition (when no more weight loss was observed) and divided by the weight at 600°C. This number is not the same as the difference in percentages obtained by directly subtracting the percentages from Fig. 5.

In each of the compositions, the DTA results show a large and sharp exothermic peak that occurs at a different temperature for each set of powders. The exothermic peak occurs at ~600°C for $BaTiO_3$, ~425°C for $Ba_{0.5}Sr_{0.5}TiO_3$, and ~500°C for $SrTiO_3$. The gradual weight loss at <600°C and exothermic peaks at temperatures below the largest peak result from removal of water, solvents, and bound organics in the systems. A small exothermic peak also occurs at ~700°C for $BaTiO_3$ and at ~600°C for $Ba_{0.5}Sr_{0.5}TiO_3$.

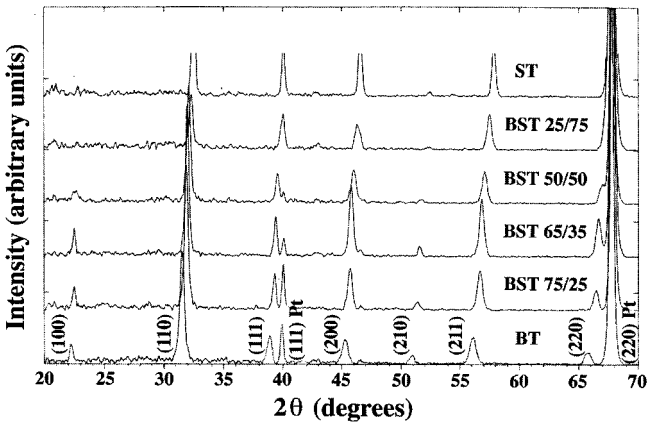

Fig. 1. Glancing-angle thin-film XRD of $Ba_xSr_{1-x}TiO_3$ films on Pt/Ti/SiO_2/Si (BT = $BaTiO_3$, ST = $SrTiO_3$, BST ratio = Ba/Sr).

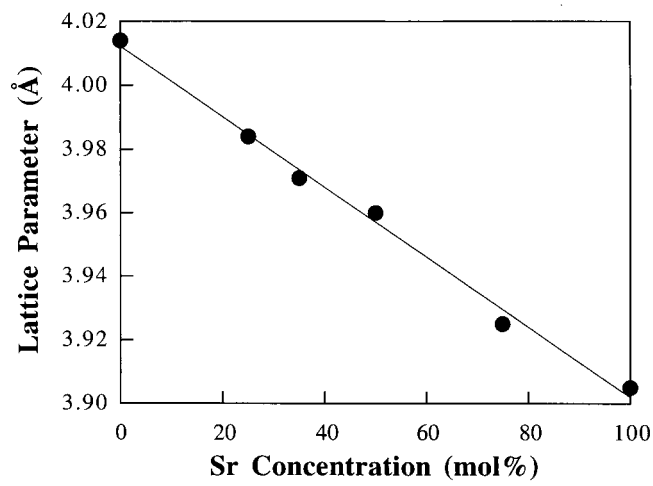

Fig. 2. Lattice parameter as a function of strontium content for $Ba_xSr_{1-x}TiO_3$ films on Pt/Ti/SiO_2/Si.

(2) In Situ TEM Studies of $Ba_{0.5}Sr_{0.5}Ti_{O3}$

The evolution of the film microstructure for $Ba_{0.5}Sr_{0.5}TiO_3$ during *in situ* TEM heating at 650°C is shown in Fig. 6. The micrographs of the cross-section TEM sample and corresponding electron diffraction patterns indicate that the film was initially amorphous (Fig. 6(a)). The amorphous film contained porosity concentrated at the interfaces between each of the film layers. The film crystallized within 10 min after reaching 650°C. Nucleation occurred both in the bulk of the gel film and along the film/platinum interface. The electron diffraction patterns (Figs. 6(b) and (c)) correspond to $Ba_{0.5}Sr_{0.5}TiO_3$, with no evidence of additional phases.

Figure 7 shows the evolution of the film microstructure at 575°C in a thin region of the film. (Here, most of the substrate was sputtered away during ion milling). The (111) oriented polycrystalline platinum substrate layer had a rough surface, with roughness on the order of 5–10 nm. Nucleation of $Ba_{0.5}Sr_{0.5}TiO_3$ was concentrated at the platinum surface, although some concurrent nucleation was noted within the bulk of the gel film. Holding the film for longer times at 575°C enhanced crystallization along the film/platinum interface.

A crystallization time sequence at 575°C, using electron diffraction patterns, is shown in Fig. 8. (The SAD patterns were taken from a region thicker than that in Fig. 7). Initially, the film was amorphous, as indicated by the diffuse halo in the diffraction pattern (Fig. 8(a)). The film crystallized after ~2 h at 575°C. However, in the halo region, a clear diffraction ring developed, with a *d* spacing of 3.22 Å, that did not match $Ba_{0.5}Sr_{0.5}TiO_3$ (Fig. 8(c)), while corresponding bright diffraction spots matched $Ba_{0.5}Sr_{0.5}TiO_3$.

IV. Discussion

(1) Effects of Strontium Concentration

The lattice parameter of $Ba_xSr_{1-x}TiO_3$ decreased linearly as the strontium concentration increased, behavior characteristic of a solid solution. The measured lattice parameters ranged from 4.014 Å for $BaTiO_3$ to 3.905 Å for $SrTiO_3$, in good agreement with the lattice parameter values for bulk perovskite $BaTiO_3$ and $SrTiO_3$. Although both $BaTiO_3$ and $Ba_{0.75}Sr_{0.25}TiO_3$ should be tetragonal at room temperature, all compositions appeared to be cubic. The

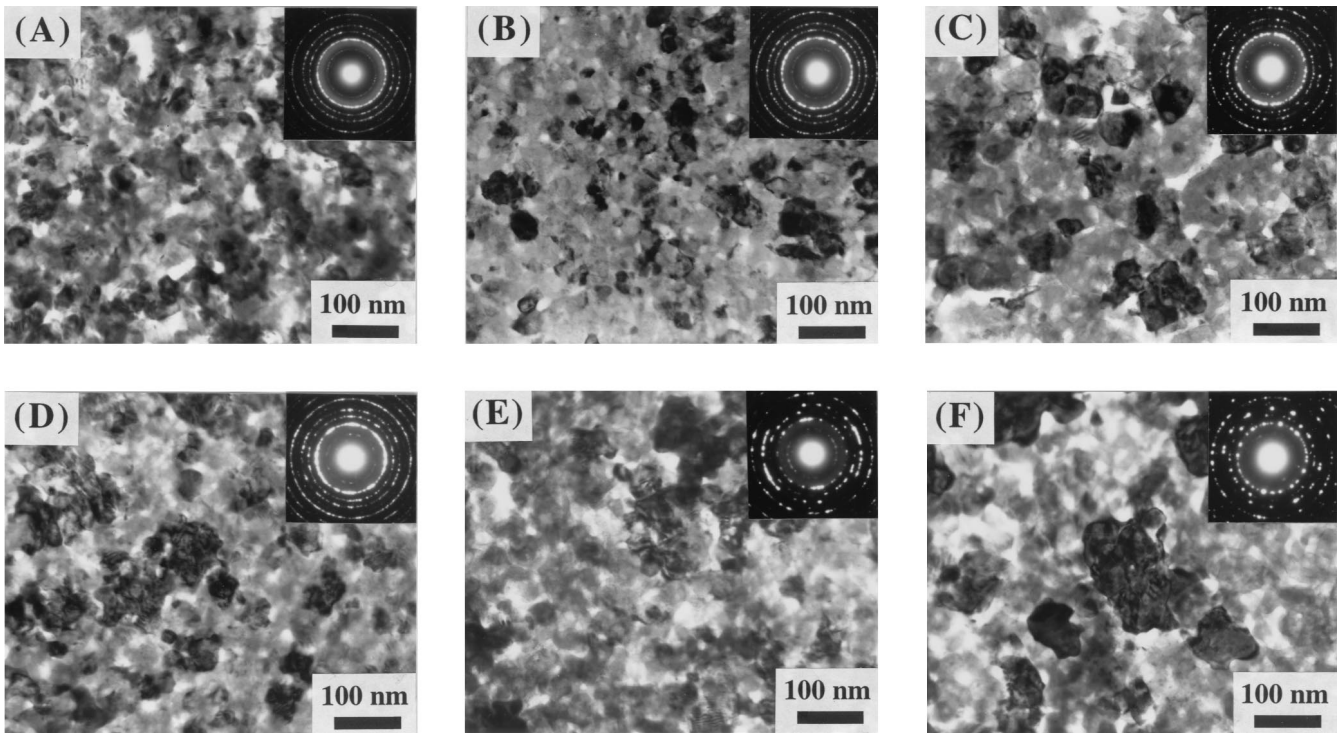

Fig. 3. Bright-field TEM micrographs and corresponding electron diffraction patterns of $Ba_xSr_{1-x}TiO_3$ films on $Pt/Ti/SiO_2/Si$ for x values of (A) 1, (B) 0.75, (C) 0.65, (D) 0.50, (E) 0.25, and (F) 0.

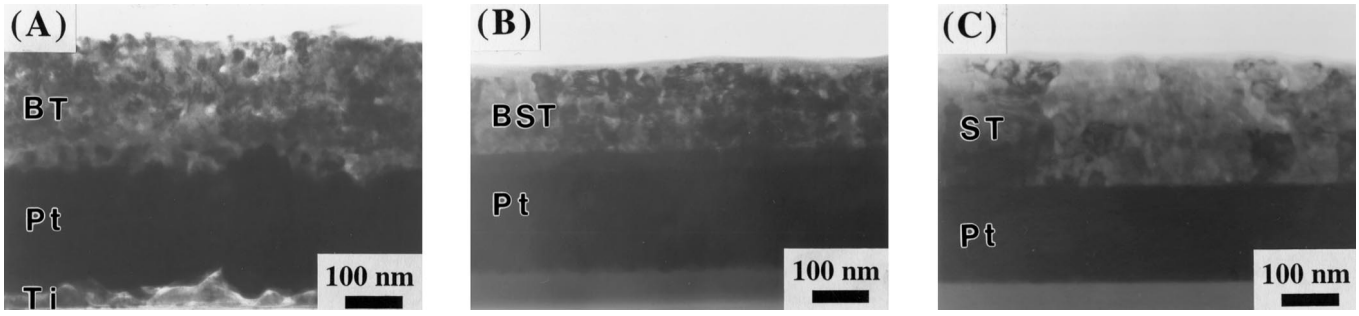

Fig. 4. Cross-section TEM micrographs of $Ba_xSr_{1-x}TiO_3$ films on $Pt/Ti/SiO_2/Si$ for x values of (A) 1, (B) 0.5, and (C) 0.

absence of tetragonality may be attributed to the fine grain size of the materials and the high volume of grain boundaries in these nanometer-grain-size films.[15,16]

The addition of strontium to the $BaTiO_3$ lattice increased the grain size of the crystallized films. The increasing grain size with increasing strontium may be attributable to higher grain-growth rates from the more rapid diffusion of the Sr^{2+} ion, which has a smaller ionic radius than Ba^{2+}. There was also a lowering of the temperature for the exothermic peaks found by DTA with increasing strontium content and a lower temperature of crystallization for the perovskite phase observed in the *in situ* experiments. Crystallization may also be initiated earlier with higher strontium contents, resulting in a larger grain size for the same heat treatment.

$SrTiO_3$ and platinum have a lattice mismatch of only ~0.5%, so increased grain size with increasing strontium concentration may result from the domination of preferred heterogeneous nucleation on the polycrystalline platinum. However, Kawano *et al.*[5] also observed an increase in grain size with increasing strontium concentration in the crystallization of free-standing films, suggesting that the increase in grain size may be related more to diffusion of Sr^{2+} and Ba^{2+} than to substrate effects.

Dielectric measurements of the various $Ba_xSr_{1-x}TiO_3$ films revealed no systematic relationship between the strontium concentration and the dielectric constant in this system.[17] The highest measured dielectric constant of 400, for the thin-film composition $Ba_{0.5}Sr_{0.5}TiO_3$, is about an order of magnitude lower than dielectric constants observed for bulk $Ba_xSr_{1-x}TiO_3$[18] but consistent with data for other $Ba_xSr_{1-x}TiO_3$ thin films of similar thickness.[14,19–21]

(2) Intermediate Phase Formation for $Ba_{0.5}Sr_{0.5}Ti_{O3}$

A previous *in situ* TEM study of methoxypropoxide-derived $BaTiO_3$ thin films revealed that amorphous gel films crystallize via the formation of an intermediate carbonate phase, believed to be $BaTiO_2CO_3$, which subsequently is transformed to $BaTiO_3$.[22] The most intense diffraction, as observed in electron diffraction patterns and XRD patterns, occurs at a d spacing of 3.32 Å. (A few additional d spacings for this phase can be observed but are much weaker.) The large exotherm of the TGA in Fig. 5 has been associated with the formation of this intermediate carbonate phase. The existence of a carbonate phase has been well-established by Fourier transform infrared spectrometry and Raman spectroscopy,[23,24] but the exact stoichiometry of the intermediate phase has been more difficult to ascertain.

This reaction,

$$BaTiO_2CO_3 \leftrightarrow BaTiO_3 + CO_2 \quad (1)$$

has a weight loss of 16%, close to the observed weight loss of 17% shown in Fig. 5(a). The reaction of $BaCO_3$ and TiO_2 also has the same weight loss as the reaction in Eq. (1):

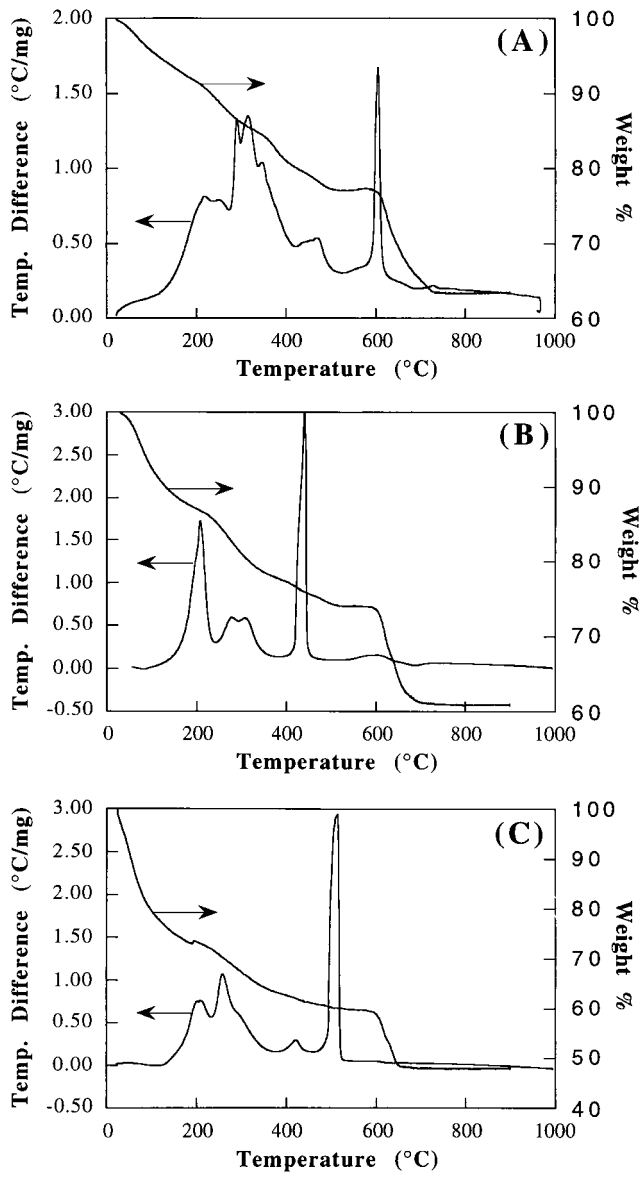

Fig. 5. DTA/TGA of dried methoxypropoxide/butanol gel powders: (A) Ba-Ti, (B) $Ba_{(0.5)}$-$Sr_{(0.5)}$-Ti, and (C) Sr-Ti.

$$BaCO_3 + TiO_2 \leftrightarrow BaTiO_3 + CO_2 \quad (2)$$

However, the *d* spacings found in XRD and electron diffraction do not exactly match $BaCO_3$ or TiO_2. Another alternative reaction that has been proposed,[23]

$$Ba_2Ti_2O_5CO_3 \leftrightarrow 2BaTiO_3 + CO_2 \quad (3)$$

gives only a 9% weight loss and is not consistent with the observed weight loss.

In metallorganic-resin-derived $SrTiO_3$, Cho *et al.*[25] observed, by XRD, an extra diffraction peak at $d = 3.13$ Å. This peak could not be assigned to a strontium titanate compound. They speculated that it was caused by an intermediate $Sr_2Ti_2O_5CO_3$ phase, because the observed weight loss of 12.4%, determined by TGA, was close to the 10.7% calculated for the decomposition of $Sr_2Ti_2O_5CO_3$. They proposed the following reaction.

$$Sr_2Ti_2O_5CO_3 \leftrightarrow 2SrTiO_3 + CO_2 \quad (4)$$

However, the weight loss in Fig. 6, associated with the decomposition reaction and the formation of $SrTiO_3$, is 18.6%, a number that matches much better the calculated 19.3% weight loss associated with the following reaction.

$$SrTiO_2CO_3 \leftrightarrow SrTiO_3 + CO_2 \quad (5)$$

In a similar fashion to Eqs. (1) and (5), the decomposition reaction

$$Ba_{0.5}Sr_{0.5}TiO_2CO_3 \leftrightarrow Ba_{0.5}Sr_{0.5}TiO_3 + 3CO_2 \quad (6)$$

has a calculated weight loss of 17.4%, matching well the experimental value of 17.5% obtained from the TGA experiments.

These observations lead to the conclusion that there is a single intermediate carbonate phase, $Ba_xSr_{1-x}TiO_2CO_3$, which is a solid solution. If this theory is true, a linear relationship should exist between the lattice parameter and the strontium concentration of the intermediate carbonate phase (similar to $Ba_xSr_{1-x}TiO_3$). This intermediate phase should have $d = 3.23$ Å for $Ba_{0.5}Sr_{0.5}TiO_2CO_3$ (halfway between the 3.32 Å of the barium titanium carbonate phase and the 3.13 Å of the strontium titanium carbonate phase). This calculation of $d = 3.23$ Å does, indeed, match closely the non-perovskite ring at $d = 3.22$ Å that was observed during *in situ* TEM heating at 575°C (Fig. 8) of a 50/50 Ba/Sr film.

These results indicate that, although the barium and strontium may be closely associated for these alkoxide solutions, unfortunately, so are the organic groups that remain in the film after low-temperature pyrolysis. These residual, bound organic groups may react with the Ba/Sr and titanium to form the undesirable carbonate phase. Crystallization of the perovskite phase is then prevented until this carbonate phase decomposes at 600°C. At >600°C, random nucleation of the perovskite phase in the bulk of the film is promoted by the high driving force for nucleation and crystallization, resulting in a relatively fine-grained microstructure.

In the examples presented here, the films are fully converted to the carbonate phase before the formation of the perovskite phase, and the decomposition reaction apparently goes nearly to completion, because the calculated weight losses for 100% decomposition closely match the observed weight losses. Other researchers[23,25] have found lower weight losses associated with the decomposition reaction than those reported here. One possibility for the difference is that the proportional release of CO_2 would be lower than that for complete combustion if the decomposition reaction were not complete. Another alternative is that specific processing routes can reduce the amount of the intermediate carbonate compound formed, giving a smaller weight loss on decomposition of the carbonate than if the entire material were carbonate. If condensation reactions are promoted, which form more oxy bridges, then the residual, bound organic concentration will be reduced. This latter argument is supported by the fact that the proposed reactions of Eqs. (3) and (4) can be rewritten as

$$BaTiO_3 + BaTiO_2CO_3 \leftrightarrow 2BaTiO_3 + CO_2 \quad (7)$$

and

$$SrTiO_3 + SrTiO_2CO_3 \leftrightarrow 2SrTiO_3 + CO_2 \quad (8)$$

which are similar to Eq. (1), with excess barium or strontium and oxygen that has not reacted to form the intermediate carbonate phase. This reaction would presumably occur if the carbon in the sample were insufficient to fully crystallize the material as the intermediate carbonate phase.

(3) Grain-Size Distribution

The large grain-size distribution in the crystallized $Ba_{0.5}Sr_{0.5}TiO_3$ thin film (Fig. 3(d)), with grains as small as 20 nm and as large as 120 nm, has also been observed by others in solution-derived $Ba_xSr_{1-x}TiO_3$.[13,26] Because the lattice mismatch between platinum and $Ba_xSr_{1-x}TiO_3$ decreases as the strontium content increases, from ~3% for cubic $BaTiO_3$ to ~0.5% for $SrTiO_3$, one explanation for the larger grain-size distribution might be competing processes between oriented growth on the platinum layer, resulting in larger grains, and nucleation in the bulk of the gel film. Sedlar *et al.*[13] have noted that larger grains form near the platinum/film interface in films subjected to multiple rapid thermal annealing (RTA) heat treatments, because of extended processing

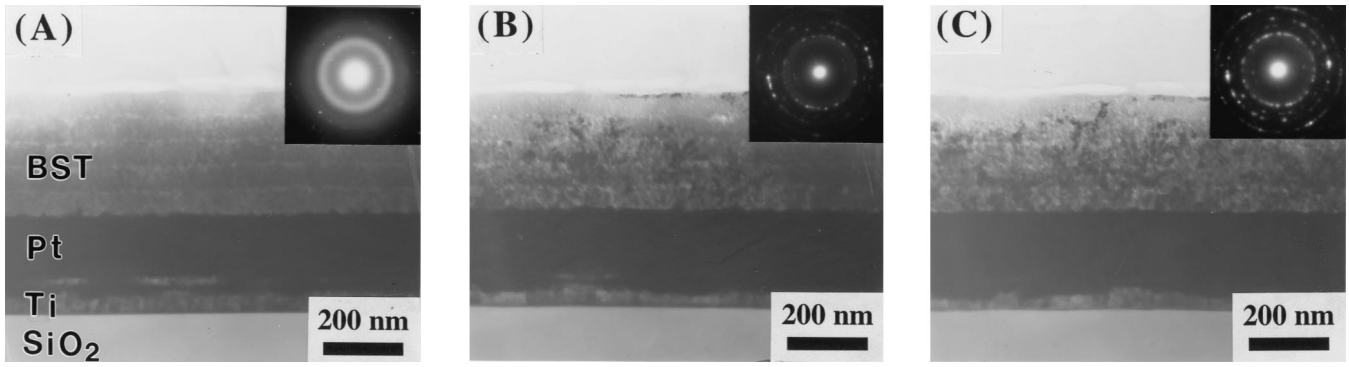

Fig. 6. Cross-section TEM micrographs of $Ba_{0.5}Sr_{0.5}TiO_3$ film on $Pt/Ti/SiO_2/Si$ after *in situ* TEM heating at 650°C for (A) 0, (B) 10, and (C) 30 min.

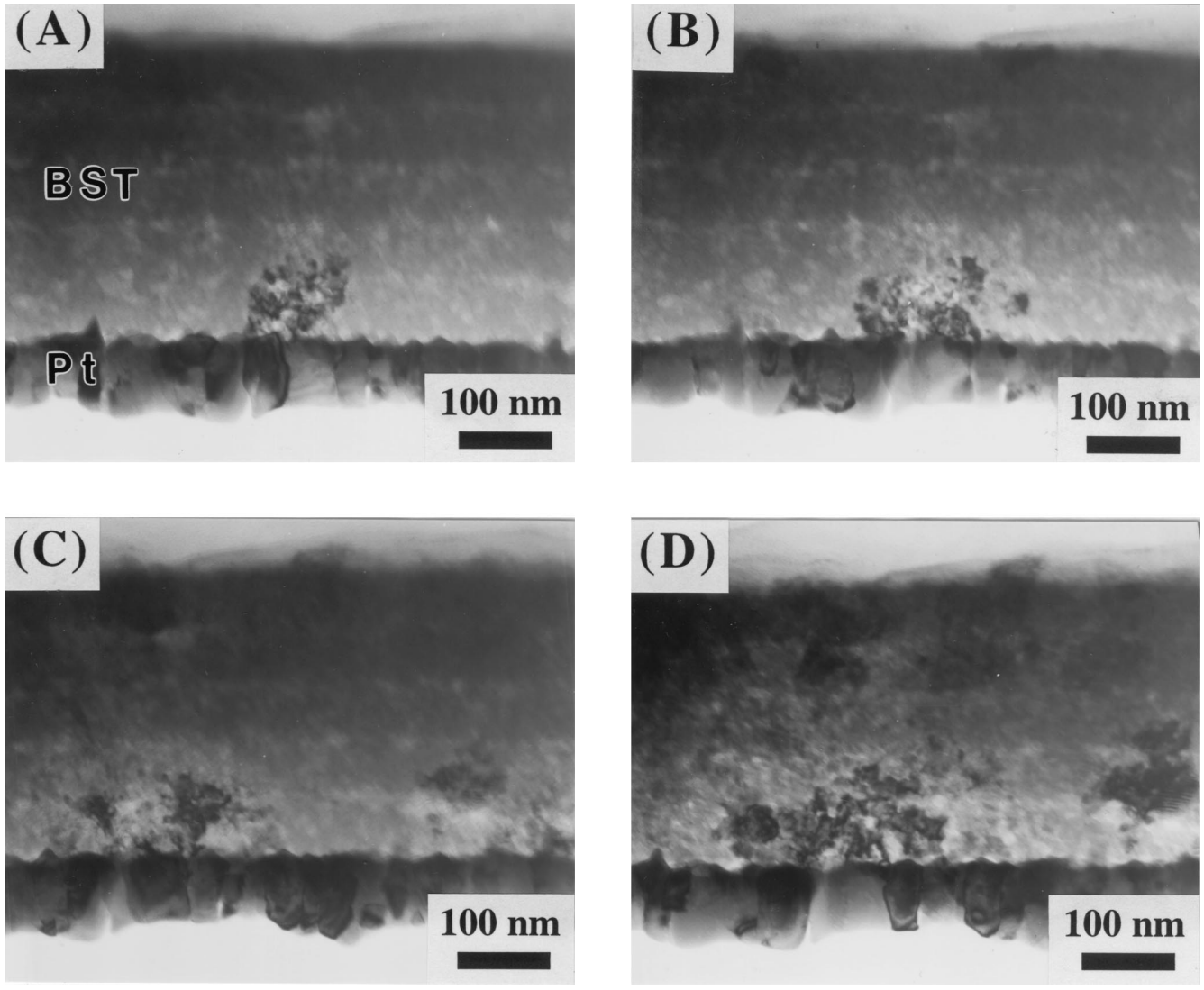

Fig. 7. Cross-section TEM micrographs of $Ba_{0.5}Sr_{0.5}TiO_3$ film on $Pt/Ti/SiO_2/Si$ after *in situ* TEM heating at 575°C for (A) 1, (B) 2, (C) 3, and (D) 5 h.

times in the layers near the interface. Some evidence can be seen for this in Fig. 4(c), with some large grains growing from the platinum substrate through the thickness of the film for the $SrTiO_3$ film. The nucleation of large grains of $Ba_{0.5}Sr_{0.5}TiO_3$ at the film/platinum interface is also evident in Fig. 7, even though all layers of the *in situ* sample of Fig. 7 were heated for the same time.

V. Conclusions

A linear relationship exists between the lattice parameter and strontium concentration for these $Ba_xSr_{1-x}TiO_3$ thin films, which form a complete solid solution from $x = 1$ to $x = 0$. There is evidence for some enhanced nucleation of $Ba_xSr_{1-x}TiO_3$ at the film/platinum interface with increasing strontium concentration and closer lattice matching. The grain size increases as the strontium content increases for these sol–gel-derived $Ba_xSr_{1-x}TiO_3$ thin films, a result attributable to the more rapid diffusion of strontium ions, compared with that of barium ions. The average grain sizes for $Ba_xSr_{1-x}TiO_3$ with $x = 1$, 0.75, 0.65, 0.50, 0.25, and 0 are ~40, 50, 60, 70, 110, and 120 nm. An intermediate phase of $Ba_xSr_{1-x}TiO_2CO_3$, also a solid solution from $x = 1$ to $x = 0$, forms before the perovskite $Ba_xSr_{1-x}TiO_3$ and decomposes at 600°C. The

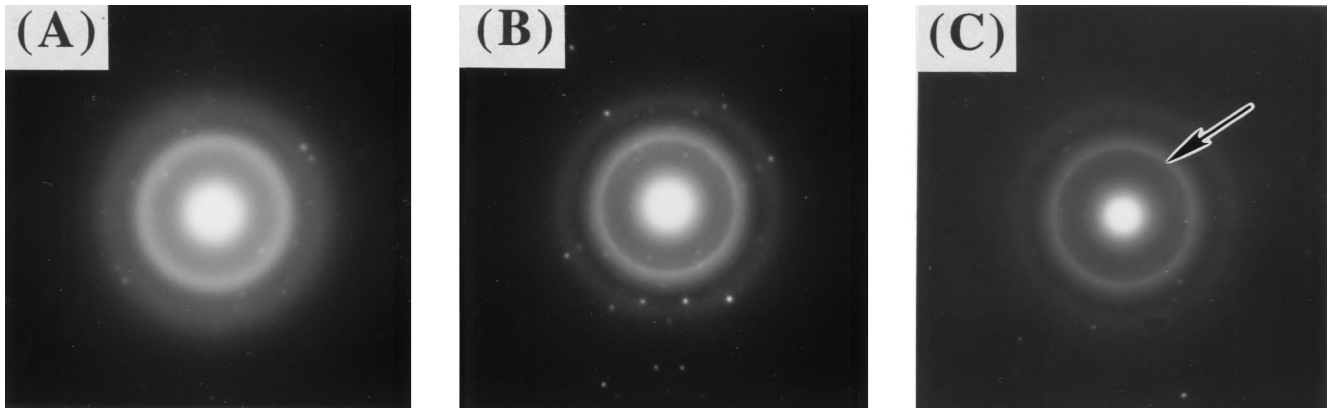

Fig. 8. Electron diffraction patterns of $Ba_{0.5}Sr_{0.5}TiO_3$ film on Pt/Ti/SiO_2/Si after *in situ* TEM heating at 575°C for (A) 0, (B) 1, and (C) 2 h (arrow points to phase at $d = 3.22$ Å).

formation of this carbonate phase inhibits the crystallization of the perovskite $Ba_xSr_{1-x}TiO_3$ at <600°C, above which temperature there is a high driving force for random nucleation and crystallization in the bulk. The present results suggest that, although it may be possible to use compositional modifications to tailor the thin-film microstructure, the detrimental presence of an intermediate carbonate phase may dominate microstructural development for this sol–gel process and hinder optimization of desired dielectric properties.

References

[1]L. H. Parker and A. F. Tasch, "Ferroelectric Materials for 64 Mb and 256 Mb DRAMs," *IEEE Circuits Devices Mag.*, **6** [1] 17–26 (1990).

[2]R. F. Pinizzotto, E. G. Jacobs, H. Yang, S. R. Summerfelt, and B. E. Gnade, "Cross-Section TEM Studies of Barium Strontium Titanate Deposited on Silicon by Pulsed Laser Ablation"; pp. 463–68 in *Ferroelectric Thin Films II*, Proceedings of the Materials Research Society Symposium (Boston, MA, Dec. 2–4, 1991). Edited by A. I. Kingon, E. R. Meyers, and B. Tuttle. Materials Research Society, Pittsburgh, PA, 1992.

[3]P. Bhattacharya, P. Kyung-Ho, and Y. Nishioka, "Control of Grain Structure of Laser-Deposited (Ba,Sr)TiO_3 Films to Reduce Leakage Current," *Jpn. J. Appl. Phys., Part 1*, **33** [9B] 5231–34 (1994).

[4]S. B. Qadri, J. S. Horwitz, D. B. Chrisey, R. C. Y. Auyeung, and K. S. Grabowski, "X-ray Characterization of Extremely High Quality (Sr,Ba)TiO_3 Films Grown by Pulsed Laser Deposition," *Appl. Phys. Lett.*, **66** [13] 1605–607 (1995).

[5]H. Kawano, K. Morii, and Y. Nakayama, "Effects of Crystallization on Structural and Dielectric Properties of Thin Amorphous Films of $(1-x)BaTiO_3-xSrTiO_3$ (x = 0–0.5, 1.0)," *J. Appl. Phys.*, **73** [10] 5141–46 (1993).

[6]K. Abe and S. Komatsu, "Ferroelectric Properties in Epitaxially Grown $Ba_xSr_{1-x}TiO_3$ Thin Films," *J. Appl. Phys.*, **77** [12] 6461–65 (1995).

[7]N. Ichinose and T. Ogiwara, "Preparation and Rapid Thermal Annealing Effect of (Ba,Sr)TiO_3 Thin Films," *Jpn. J. Appl. Phys., Part 1*, **34** [9B] 5198–201 (1995).

[8]C. S. Chern, S. Liang, Z. Q. Shi, S. Yoon, A. Safari, P. Lu, B. H. Kear, B. H. Goodreau, T. J. Marks, and S. Y. Hou, "Heteroepitaxial Growth of $Ba_{1-x}Sr_xTiO_3$/$YBa_2Cu_3O_{7-x}$ by Plasma-Enhanced Metalorganic Chemical Vapor Deposition," *Appl. Phys. Lett.*, **64** [23] 3181–83 (1994).

[9]A. B. Catalan, J. V. Mantese, A. L. Micheli, N. W. Schubring, and R. J. Poisson, "Preparation of Barium Strontium Titanate Thin Film Capacitors on Silicon by Metallorganic Decomposition," *J. Appl. Phys.*, **76** [4] 2541–43 (1994).

[10]Y. Wu, E. G. Jacobs, R. F. Pinizzotto, R. Tsu, H.-Y. Liu, S. R. Summerfelt, and B. E. Gnade, "Microstructural and Electrical Characterization of Barium Strontium Titanate Thin Films"; pp. 269–74 in *Ferroelectric Thin Films IV*, Proceedings of the Materials Research Society Symposium (Boston, MA, Nov. 29–Dec. 2, 1994). Edited by B. A. Tuttle, S. B. Desu, R. Ramesh, and T. Shiosaki. Materials Research Society, Pittsburgh, PA, 1995.

[11]T. Hayashi and T. Tanaka, "Preparation and Dielectric Properties of $SrTiO_3$/$BaTiO_3$ Multilayer Thin Films by Sol–Gel Method," *Jpn. J. Appl. Phys., Part 1*, **34** [9B] 5100–104 (1995).

[12]J. Kim, S. I. Kwun, and J. G. Yoon, "Precursor Dependent Properties of $Ba_{1-x}Sr_xTiO_3$ Thin Films Fabricated by Sol–Gel Method"; pp. 423–26 in *ISAF '94*, Proceedings of the 9th IEEE International Symposium on Applications of Ferroelectrics (University Park, PA, Aug. 7–10, 1994). Edited by R. K. Pandey, M. Liu, and A. Safari. IEEE, New York, 1994.

[13]M. Sedlar, M. Sayer, and L. Weaver, "Sol–Gel Processing and Properties of Cerium Doped Barium Strontium Titanate Thin Films," *J. Sol–Gel Sci. Technol.*, **5** [3] 201–10 (1995).

[14]D. M. Tahan, A. Safari, and L. C. Klein, "Preparation and Characterization of $Ba_xSr_{1-x}TiO_3$ Thin Films by a Sol–Gel Technique," *J. Am. Ceram. Soc.*, **79** [6] 1593–98 (1996).

[15]M. H. Frey and D. A. Payne, "Nanocrystalline Barium Titanate: Evidence for the Absence of Ferroelectricity in Sol–Gel-Derived Thin-Layer Capacitors," *Appl. Phys. Lett.*, **63** [20] 2753–55 (1993).

[16]G. Arlt, D. Hennings, and G. de With, "Dielectric Properties of Fine-Grained Barium Titanate Ceramics," *J. Appl. Phys.*, **58** [4] 1619–25 (1985).

[17]M. C. Gust, L. A. Momoda, and M. L. Mecartney, "Influence of Strontium Concentration on the Microstructure and Electrical Properties of Sol–Gel Derived Barium Strontium Titanate Thin Films"; pp. 27–32 in *Ferroelectric Thin Films V*, Proceedings of the Materials Research Society Symposium (San Francisco, CA, Apr. 8–12, 1996). Edited by S. Desu, R. Ramesh, B. Tuttle, R. Jones, and I. Yoo. Materials Research Society, Pittsburgh, PA, 1996.

[18]U. Syamaprasad, R. K. Galgali, and B. C. Mohanty, "Dielectric Properties of the $Ba_{1-x}Sr_xTiO_3$ System," *Mater. Lett.*, **7** [5,6] 197–200 (1988).

[19]R. Tsu, L. Hung-Yu, H. Wei-Yung, S. Summerfelt, K. Aoki, and B. Gnade, "Correlations of $Ba_{1-x}Sr_xTiO_3$ Materials and Dielectric Properties"; see Ref. 10, pp. 275–80.

[20]S. Yamamichi, T. Sakuma, T. Hase, and Y. Miyasaka, "$SrTiO_3$ and (Ba,Sr)TiO_3 Thin Films Preparation by Ion Beam Sputtering and Their Dielectric Properties"; see Ref. 2, pp. 297–302.

[21]D. M. Tahan, A. Safari, and L.C. Klein, "Processing and Dielectric Properties of Sol–Gel Derived BST Thin Films," *Integr. Ferroelectr.*, **15** [1–4] 99–106 (1996).

[22]M. C. Gust, N. D. Evans, L. A. Momoda, and M. L. Mecartney, "*In Situ* Transmission Electron Microscopy Crystallization Studies of Barium Titanate Thin Films," *J. Am. Ceram. Soc.*, **80** [11] 2828–36 (1997).

[23]S. Kumar, G. L. Messing, and W. B. White, "Metal Organic Resin Derived Barium Titanate: I, Formation of Barium Titanium Oxycarbonate Intermediate," *J. Am. Ceram. Soc.*, **76** [3] 617–24 (1993).

[24]M. H. Frey and D. A. Payne, "Synthesis and Processing of Barium Titanate Ceramics from Alkoxide Solutions and Monolithic Gels," *Chem. Mater.*, **7**, 123–29 (1995).

[25]S. G. Cho, P. F. Johnson, and R. A. Condrate, "Thermal Decomposition of (Sr,Ti) Organic Precursors during the Pechini Process," *J. Mater. Sci.*, **25**, 4738–44 (1990).

[26]D. Ivanov, M. Caron, L. Ouellet, S. Blain, N. Hendricks, and J. Currie, "Structural and Dielectric Properties of Spin-On Barium–Strontium Titanate Thin Films," *J. Appl. Phys.*, **77** [6] 2666–71 (1995). □